Redox Biology 49 (2022) 102227

Contents lists available at ScienceDirect

Redox Biology

journal homepage: www.elsevier.com/locate/redox

Induction of autophagy via the ROS-dependent AMPK-mTOR pathway protects copper-induced spermatogenesis disorder

Hongrui Guo [a,b,1], Yujuan Ouyang [a,1], Heng Yin [a,1], Hengmin Cui [a,b,c,*], Huidan Deng [a,b,**], Huan Liu [a], Zhijie Jian [a], Jing Fang [a,b], Zhicai Zuo [a,b], Xun Wang [a,b], Ling Zhao [a,b], Yanqiu Zhu [a], Yi Geng [a], Ping Ouyang [a]

[a] College of Veterinary Medicine, Sichuan Agricultural University, Wenjiang, Chengdu, 611130, China
[b] Key Laboratory of Animal Diseases and Environmental Hazards of Sichuan Province, Sichuan Agriculture University, Wenjiang, Chengdu, 611130, China
[c] Key Laboratory of Agricultural Information Engineering of Sichuan Province, Sichuan Agriculture University, Yaan, Sichuan, 625014, China

ARTICLE INFO

Keywords:
$CuSO_4$
Autophagy
Oxidative stress
Apoptosis
Spermatogenesis disorder

ABSTRACT

Copper (Cu) is a necessary micronutrient at lower concentration, while excessive Cu exposure or Cu homeostasis disorders can lead to toxicity. The mechanism of male reproductive toxicity induced by Cu is still unknown. This study aims to investigate whether autophagy plays an important role in copper-induced spermatogenesis disorder *in vivo* and vitro. The present study showed that copper sulfate ($CuSO_4$) might significantly promote autophagy level in the testis and mouse-derived spermatogonia cell line GC-1 spg cells. Concurrently, $CuSO_4$ could induce autophagy via AMPK-mTOR pathway that downregulated *p*-mTOR/mTOR and subsequently upregulated *p*-AMPKα/AMPKα as well as *p*-ULK1/ULK1. In the meanwhile, $CuSO_4$ treatment could also increase expression levels of the autophagy-related proteins. Then, the role of oxidative stress in $CuSO_4$-induced autophagy was investigated. The findings demonstrated that oxidative stress inhibitor (NAC) attenuated $CuSO_4$-induced autophagy *in vivo* and *vitro*, reversing the activation for AMPK-mTOR pathway. Additionally, the study also investigated how autophagy worked under the spermatogenesis disorder induced by $CuSO_4$. Inhibition of autophagy could decrease cell viability, and enhance the ROS accumulation and apoptosis in the GC-1 cells, meanwhile, the spermatogenesis disorder, oxidative stress and histopathological changes were increased in the testis. Furthermore, co-treatment with the apoptosis inhibitor (Z-VAD-FMK) could decrease the spermatogenesis disorder but not influence autophagy. Besides, the crosslink between autophagy and ferroptosis were also measured, the data showed that inhibition of autophagy could suppress $CuSO_4$-induced ferroptosis in *in vivo* and *vitro*. Altogether, abovementioned results indicated that $CuSO_4$ induced autophagy via oxidative stress-dependent AMPK-mTOR pathway in the GC-1 cells and testis, and autophagy activation possibly led to the generation of protection mechanism through oxidative damage and apoptosis inhibition, however, autophagy also aggravate $CuSO_4$ toxicology through promoting ferroptosis. Overall, autophagy plays a positive role for attenuating $CuSO_4$-induced testicular damage and spermatogenesis disorder. Our study provides a possible targeted therapy for Cu overload-induced reproduction toxicology.

1. Introduction

Copper (Cu) refers to an essential trace element of humans and animals as the co-factor of proteins and enzymes required by diverse physiological reactions in the organic biological system [1]. The requirement of Cu in human and animals is extremely low, and thus, Cu

; AMPK, adenosine 5′-monophosphate (AMP)-activated protein kinase; mTOR, mammalian target of rapamycin; ULK1, unc-51-like kinase 1; GPX4, glutathione peroxidase 4; FTH1, ferritin heavy chain; NCOA4, nuclear receptor coactivator 4; MAC, N-acetylcysteine; 3-MA, 3-Methyladenine; Z-VAD-FMK, N-benzyloxycarbonyl-Val-Ala-Asp-fluoromethyl-ketone; EMT, epithelial-mesenchymal transition.

* Corresponding author. College of Veterinary Medicine, Sichuan Agricultural University, Yaan, Sichuan, 625014, China.
** Corresponding author. College of Veterinary Medicine, Sichuan Agricultural University, Yaan, Sichuan, 625014, China.
E-mail addresses: chm2020@sicau.edu.cn (H. Cui), denghuidan@sicau.edu.cn (H. Deng).
[1] These authors contributed equally to this work.

https://doi.org/10.1016/j.redox.2021.102227
Received 29 November 2021; Received in revised form 25 December 2021; Accepted 29 December 2021
Available online 30 December 2021

accumulation exceeding metabolic requirements or Cu homeostasis disorder may result in toxic effects [2]. Epidemiological research has demonstrated Cu may be released into the surroundings from lots of sources in industrial and agricultural activities. Cu pollution in river has been reported all over the world. Moreover, evidence shows that excessive Cu can give rise to severe detrimental influences on the health of animals and plants, resulting in multiple organ failure [2].

Excessive Cu is likely to trigger severe detrimental influences on health, including immunotoxicity, haematotoxicity, pulmonary toxicity, hepatotoxicity, nephrotoxicity as well as neurotoxicity [3–6]. According to the former research results, Cu induces hepatotoxicity such as oxidative stress, apoptosis as well as inflammation [7,8]. $CuSO_4$ treatment causes pulmonary fibrosis via TGF-β1/Smad pathway- and MAPKs pathway-induced activation of EMT [3], and oxidative stress, apoptosis as well as inflammation [9]. Besides, more than 10 mg/kg $CuSO_4$ will trigger oxidative stress, apoptosis, DNA damage, as well as inflammation in mice spleen [4].

Recently, the research shows that excessive exposure to Cu may trigger reproduction toxicity, however, the exactly mechanism still remains unclear. Wang et al. [10] have reported that environmental exposure to Cu may exert detrimental effects on human reproductive health, including impaired semen quality, spermatozoa apoptosis and damaged sperm DNA. And high levels of Cu could decrease the sperm cells count progressively motile sperm cells after 1 h in fertile male volunteers from the southern region of Poland [11]. Moreover, the results of Li et al. [12] also have demonstrated that seminal plasma Cu values also displayed a negative correlation with normomorph sperm rate in men from Cu pollution area. Roychoudhury et al. [13,14] report the impairment of male fertility during $CuSO_4$ treatment, involving the reduction of spermatozoa concentration, viability, and motility in the rabbit. Zhang et al. [15] prove Cu accumulation within the testis, and discover that serum testosterone (T) and luteinizing hormone (LH) levels of mice show a significant fall following intraperitoneal injection with $CuCl_2$ (2.5–5 mg/kg). According to our former studies, $CuSO_4$ can induce spermatogenesis disorder, which has a connection with DNA damage and germ cell apoptosis mediated by oxidative stress [16].

Autophagy, acknowledged to be a famous conserved self-cannibalization mechanism, is playing an important part during biogenic process to acclimatize intracellular and extracellular environment changes [17]. Whereas, abnormal autophagy is potentially induced by specific abnormal stimuli and stresses, thus causing damage. The autophagy process consists of four crucial pathways: initiation, nucleation, maturation, and degradation [18]. In many stress, autophagy and apoptosis are all induced and control the cell survive or death. In general, autophagy can block apoptosis induction. Whereas, under certain circumstances, autophagy possibly induces apoptosis or necrosis, and it is also proved to cause autophagic cell death through excessively degrading the cytoplasm [17]. Our former research has also shown that excessive Cu may enhance hepatocyte autophagy [19]. Li et al. [20] have demonstrated that autophagy processes is obtained in Cu-induced myocardium injury. At the same time, chronic exposure to Cu may trigger autophagy of kidney in mice [21].

Up to now, it has been verified excessive Cu can cause testicular injury, while the exact mechanism is still unknown yet. And, it is not known whether autophagy is involved in Cu-induced spermatogenesis disorder. Therefore, the current work will generate the $CuSO_4$ intoxication model in the testis of mice and the mouse-derived spermatogonia cell line GC-1 spg cells, and then confirm the induction of autophagy and the potential mechanism of $CuSO_4$-induced autophagy. At the same time, autophagy's role in the spermatogenesis disorders induced by Cu and the association of autophagy, oxidative stress, apoptosis and ferroptosis are studied by this research.

2. Materials and methods

2.1. Materials and reagents

$CuSO_4$ came from Chengdu Kelong Chemical Co., Ltd. (Chengdu, China). N-acetylcysteine (NAC) (A9165) and 3-MA (M9281) were provided by Sigma Aldrich. Z-VAD-FMK (C1202) and 2′,7′-dichlorofluorescin diacetate (DCFH-DA) (S0033 M) were provided by Beyotime Biotechnology. Compound C (Com C) (S7306) was purchased from Selleck.

Antibodies involved in the current research included: rabbit anti-LC3B (2775S CST), rabbit anti-p62 (5114S CST), rabbit anti-AMPKα (5832 CST), rabbit anti-*p*-AMPKα (2535 CST), rabbit anti-mTOR (2972 CST), rabbit anti-*p*-mTOR (2971 CST), rabbit anti-ULK1 (8054 CST), rabbit anti-*p*-ULK1(Ser757) (6888 CST), rabbit anti-Atg16L1 (8089T CST), rabbit anti-Atg7 (8558 CST), rabbit anti-Atg3 (3415 CST), rabbit anti-Beclin1 (12994 CST), anti-rabbit cleaved-caspase-3 (9664 CST), anti-rabbit cleaved-caspase-8 (9496 CST), anti-rabbit cleaved-caspase-9 (9509 CST), anti-rabbit caspase-12 (ab18766 Abcam), and anti-rabbit cleaved-PARP (5625 CST), anti-rabbit GPX4 (ab125066 Abcam), anti-rabbit COX-2 (abs131986 Absin Biotechnology), anti-rabbit FTH1 (bs-5907R Bioss Biotechnology) and anti-rabbit NCOA4 (DF4255 Affinity biosciences).

2.2. Animals and treatments

In the present study, 240 healthy male ICR mice (8 weeks old) came from Experimental Animal Corporation of Dossy (Chengdu, China). These mice had 1-week acclimatization and were provided with sufficient water and food. The mice were classified into 4 groups at random (n = 60 each). Intragastric doses of distilled water were given to the control group, and intragastric doses of $CuSO_4$ (10, 20 or 40 mg/kg) were provided for the experimental group. Following the treatment for 21 and 42 days, mice needed to be executed for collecting testis samples required by follow-up analysis.

For investigating the effects of oxidative stress on autophagy induced by $CuSO_4$, we co-treated oxidative stress inhibitor NAC with $CuSO_4$. 32 healthy male ICR mice (8 weeks old) were classified into 4 groups at random. In terms of control group, mice received intragastric doses of distilled water and intraperitoneal injection with PBS. For $CuSO_4$ alone group, mice received intragastric doses of $CuSO_4$ (40 mg/kg) and intraperitoneal injection with PBS. For NAC alone group, mice received intragastric doses of distilled water and intraperitoneal injection with NAC (100 mg/kg body weight/day). For NAC + $CuSO_4$ group, mice had intraperitoneal injection with NAC (100 mg/kg body weight/day) 3h after the intragastric doses of $CuSO_4$ (40 mg/kg). Following treatment for 42 days, mice needed to be executed for collecting testis samples required by follow-up analysis.

For investigating the effects of autophagy on spermatogenesis disorder induced by $CuSO_4$, the autophagy inhibitor 3-MA was co-treated with $CuSO_4$ according to reference [22] and a pilot experiment. 32 healthy male ICR mice (8 weeks old) were classified into 4 groups at random. For control group, mice received intragastric doses of distilled water and intraperitoneal injection with PBS. For $CuSO_4$ alone group, mice received intragastric doses of $CuSO_4$ (40 mg/kg) and intraperitoneal injection with PBS. For 3-MA alone group, mice received intragastric doses of distilled water and intraperitoneal injection with 3-MA (30 mg/kg body weight/day). For 3-MA + $CuSO_4$ group, mice received intraperitoneal injection with 3-MA (30 mg/kg body weight/day) 30 min after intragastric doses of $CuSO_4$ (140 mg/kg). Following treatment for 3 days, mice needed to be executed 24 h after the final treatment for collecting testis samples required by follow-up analysis.

For investigating the role of apoptosis in spermatogenesis disorders induced by $CuSO_4$, the apoptosis inhibitor Z-VAD-FMK was co-treated with $CuSO_4$. 32 healthy male ICR mice (8 weeks old) were randomly classified into 4 groups. For control group, mice received intragastric

doses of distilled water and intraperitoneal injection with PBS. For $CuSO_4$ alone group, mice received intragastric doses of $CuSO_4$ (40 mg/kg) and intraperitoneal injection with PBS. For Z-VAD-FMK alone group, mice received intragastric doses of distilled water and intraperitoneal injection with Z-VAD-FMK (10 mg/kg body weight/day). For Z-VAD-FMK + $CuSO_4$ group, mice had intraperitoneal injection with Z-VAD-FMK (10 mg/kg body weight/day) 30 min after intragastric doses of $CuSO_4$ (140 mg/kg). Following treatment for 3 days, mice needed to be executed 24 h after the final treatment for collecting testis samples required by follow-up analysis.

Each mouse was utilized in the current experiment. This experimental protocol obtained approval from the Animal Care and Use Committee of Sichuan Agricultural University (Chengdu, China).

2.3. Cell culture

Mouse GC-1 spg cells were cultured in DMEM with 10% fetal bovine serum (FBS) supplementing 0.1 mg/ml streptomycin and 100 IU/ml penicillin, and incubated at the conditions of 37 °C, 5% CO_2. The cells were subcultured as the cell growth density reached about 80% to ensure cell nutrition and keep cells in the logarithmic growth phase.

2.4. MTT assay

Mouse GC-1 spg cells were plated onto a 96-well plate with a number of 1×10^4 cells per well. The cells were treated with 0, 0.4, 0.8 or 1.6 mM $CuSO_4$ for 12 or 24 h or treated with 0 or 1.6 mM for 24 h in the presence or absence of NAC (5 mM) or 3-MA (1 mM) or Z-VAD-FMK (20 μM). Cell viability was measured with the addition of MTT, and the absorbance was determined by using a spectrophotometer at 490 nm.

2.5. Sperm quality

Epididymal sperm needed to be suspended in normal saline at 37 °C for suspension preparation. Subsequently, the approach developed in Ommati et al. [23] had been chosen for measuring the number of sperms.

2.6. Pathological observations

Mice were executed for collecting testis samples. Afterwards, every sample needed to receive 4% paraformaldehyde fixation, gradient ethanol dehydration and paraffin embedding. Then, these samples were cut into slices (with a thickness of 4 μm) and dyed by hematoxylin and eosin (H&E). With optical microscope, histopathological symptoms could be detected.

2.7. Determination of oxidative damage and antioxidant parameters

Testis samples were washed within chilled saline solution, weighed and homogenized with nine volumes of ice-cold 0.9% NaCl solution, followed by centrifugation at 3500 rpm for 10 min at 4 °C. By inserting the supernatant to new eppendorf tubes, the content of T-AOC (Cat. No. A015), SOD (Cat. No. A001-1), CAT (Cat. No. A007-1), GSH-Px (Cat. No. A005), GSH (Cat. No. A061-1), as well as MDA (Cat. No. A003-1) was investigated using the commercially available kits (Nanjing Jiancheng Bioengineering Institute, Nanjing, China) in accordance with the specifications.

2.8. Apoptosis analysis by flow cytometry

GC-1 spg cells were treated with $CuSO_4$, and washed by the pre-chilled PBS (pH 7.2–7.4), followed by suspension within PBS to 1 × 106 cells/ml. Briefly, the 5 ml tube was added with 100 μL cell suspension, followed by 15 min Annexin V- FITC (5 μL, Cat: 51-65874X, BD, USA) and PI (5 μL, Cat: 51-66211E, BD, USA) staining under 25 °C in dark. After the addition of 1 × binding buffer (400 μl), the flow cytometry (BD FACS Calibur) was used to assess stained cells in 40 min after they were prepared. In addition, the ModFit LT v3.0 software was employed to analyze the flow cytometric data.

2.9. ROS detection by fluorescence staining

The ROS was measured using DCFH-DA. Briefly, GC-1 cells were treated $CuSO_4$ with/without NAC or 3-MA. After washing by PBS twice, cells were subjected to 10 min incubation using the 20 μM DCFH-DA for 20 min. Then, cells were rinsed by PBS twice and fixed with 4% paraformaldehyde. All images were acquired with a fluorescence microscope.

2.10. ROS detection by flow cytometry

GC-1 spg cells were treated $CuSO_4$ with/without NAC or 3-MA, and washed by the pre-chilled PBS (pH 7.2–7.4), followed by suspension within PBS to 1×10^6 cells/ml. Briefly, the 5 ml tube was added with 300 μL cell suspension, followed by 20 min DCFH-DA (20 μM) staining. After washing with PBS, cells were centrifuged at 600×*g* for 5 min. Then, supernatants were discarded, cells were resuspended in 0.5 mL PBS, and BD FACS Calibur flow was adopted for determining cell number.

2.11. Western blotting

Testes needed to be lysed in the pre-chilled RIPA buffer. Afterwards, cell lysate was centrifugated for 15 min at 15000 g and 4 °C. 12% SDS-PAGE was made for separating proteins, with subsequent transfer to PVDF membranes. Afterwards, 5% non-fat milk dissolved in TBST was employed for blocking membranes, followed by incubation by using primary antibodies as well as HRP-labeled secondary antibodies successively. The ECL detection kit (GE Healthcare, Piscataway, NJ, USA) was used in visualization. The protein bands could be visualized with Bio-Rad ChemiDoc XRS+ System (Bio-Rad Laboratories, Inc., Hercules, CA, USA). ImageJ2x software had been adopted for determining the significant difference in protein expression.

2.12. RNA extraction and quantitative real-time PCR (qRT-PCR)

RNAiso Plus (9109; Takara, China) was chosen in total RNA extraction according to the manufacturer's protocol. cDNA synthesis was made with RNA (1 μg) in combination with the Prim-ScriptTM RT reagent Kit (RR047A, Takara, China) in accordance with corresponding specifications. The gene data came from National Center for Biotechnology Information (NCBI), and Sangon (Shanghai, China) took charge of primer design and synthesis. The mRNA expression was assessed using SYBR® Premix Ex TaqTMII (RR820A, Takara, China) according to corresponding specifications. All the reactions needed to be performed at 95 °C for 10 min, and then at 95 °C for 10 min, at 60 °C for 20 s, and at 72 °C for 20 s. Subsequently, melt curves were investigated to identify PCR specificity. Additionally, the results of qRT-PCR were analyzed using the $2-\Delta\Delta CT$ method [24]. Table 1 showed qRT-PCR primers.

2.13. Determination of iron content in the liver

Testes tissues were weighed and homogenized with 9-fold volume of normal saline, then followed by centrifugated at 4 °C for 10min at 3500 rpm, the supernatant was collected. Iron content was investigated using the commercially available kits (A039-2-1, Nanjing Jiancheng Bioengineering Institute, Nanjing, China) in accordance with the specifications.

2.14. Statistical analysis

The results had been illustrated by mean ± SD. One-way ANOVA was chosen for comparing significant differences between control group and

Table 1
Sequence of primers used in qRT-PCR.

Target gene	Accession number	Primer	Primer sequence (5′–3′)	Product size	*Tm* (°C)
CuZn-SOD	NM-011434	Forward	GGGTTCCACGTCCATCAGTA	113bp	56.8
		Reverse	CAGGTCTCCAACATGCCTCT		
Mn-SOD	NM-013671	Forward	AACTCAGGTCGCTCTTCAGC	113bp	59.3
		Reverse	CTCCAGCAACTCTCCTTTGG		
CAT	NM-009804	Forward	CCTATTGCCGTTCGATTCTC	119bp	58.6
		Reverse	CCCACAAGATCCCAGTTACC		
GSH-Px	NM_008160	Forward	TACACCGAGATGAACGATCTG	102bp	60.2
		Reverse	ATTCTTGCCATTCTCCTGGT		
Beclin1	NM-019584	Forward	TGCAGGTGAGCTTCGTGTG	124bp	58.6
		Reverse	GCTCCTCTCCTGAGTTAGCCT		
Atg12	NM-026217	Forward	TAAACTGGTGGCCTCGGAAC	146bp	60.2
		Reverse	ATCCCCATGCCTGGGATTTG		
Atg5	NM-053069	Forward	CAAGGATGCGGTTGAGGC	167bp	58.8
		Reverse	TGAGTTTCCGGTTGATGG		
Atg16L1	NM-001205392	Forward	CTGAGAAGGCCCAAGAAGCC	221bp	58.5
		Reverse	GACAGAGCGTCTCGTAGCTG		
Atg7	NM_001253718	Forward	TCGAAAACCCCATGCTCCTC	175bp	59.4
		Reverse	AGGGCCTGGATCTGTTTTGG		
Atg3	NM_026402	Forward	TGAAGGGAAAGGCTCTGGAAG	141bp	57.4
		Reverse	ATTGCCATGTTGGACAGTGGT		
β-actin	NM-007393	Forward	GCTGTGCTATGTTGCTCTAG	117bp	60.9
		Reverse	CGCTCGTTGCCAATAGTG		

experimental group with SPSS17.0. $P < 0.05$ suggested the value was statistically significant.

3. Results

3.1. $CuSO_4$ induced alterations in testicular structure

According to Fig. 1a, $CuSO_4$ resulted in the histopathological alterations of testis, and the histopathological alterations were time-and dose-dependent ($CuSO_4$ treatment) increased. Spermatogonia and spermatocytes experienced a significant fall. Spermatogenic cells experienced vacuolar degeneration and necrosis.

To determine the $CuSO_4$-targeted germ cells, we counted the number of spermatogonia, spermatocytes, round spermatids and elongated spermatids in per testis. There was no significant change in the number of spermatogonia (Fig. 1b). As indicated by the results, spermatocytes were remarkably reduced ($p < 0.01$) in three $CuSO_4$ treatment groups on the 21st and 42nd days during this experiment in contrast to the control group (Fig. 1c). The numbers of round spermatids were apparently declined ($p < 0.05$ or < 0.01) in 40 mg/kg treatment on the 21st day and in three $CuSO_4$ treatments on the 42nd day (Fig. 1d). Compared with the control group, elongated spermatids remarkably reduced ($p < 0.01$) in 20 and 40 mg/kg treatments on the 21st day and in three $CuSO_4$ treatments on the 42nd day of the experiment (Fig. 1e). And, the ratio of elongated spermatids to round spermatids was also remarkably reduced ($p < 0.01$) in three $CuSO_4$ treatment groups on the 21st and 42nd days during this experiment compared with the control group (Fig. 1f).

3.2. $CuSO_4$ induced autophagy through the AMPK-mTOR signaling

In this study, we explored whether autophagy was playing a role in testicular damages induced by $CuSO_4$. The LC3 conversion and p62 degradation are the crucial biomarkers of autophagy. In Fig. 2 a and b, the LC3-II/LC3-I ratio remarkably grew ($p < 0.01$) in the 40 mg/kg group on the 21st day and in three $CuSO_4$ treatment groups on the 42nd day. In addition, p62 protein expression levels experienced a significant increase ($p < 0.01$) in the 20 and 40 mg/kg groups on the 21st day and in three $CuSO_4$ groups on the 42nd day in contrast to the control group. Above results indicated that $CuSO_4$ could induce autophagy in the testis.

Under external stimuli, the AMPK-mTOR signal transduction pathway is playing a crucial role in cell autophagy. To explore how AMPK-mTOR affected $CuSO_4$-induced autophagy in the testis, the current research used western blotting in the measurement of crucial proteins associated with AMPK-mTOR signal transduction pathway. According to Fig. 2c, d and f, *p*-AMPK, *p*-mTOR and *p*-ULK1 protein expression levels remarkably enhanced on the 21st and 42nd days in comparison with the control group. In addition, the experiment also measured proteins related to autophagy flux. In accordance with the findings, Beclin1, Atg5-Atg12, Atg7, Atg3 and Atg16L1 protein expression levels experienced a significant increase in $CuSO_4$-treated groups in this experiment (Fig. 3a–f). Simultaneously, the experiment detected the mRNA expression levels in aforementioned autophagy-linked proteins. The mRNA expression levels in Beclin1 and Atg12 experienced a significant increase ($p < 0.05$ or $p < 0.01$) in $CuSO_4$-treated groups (Fig. 3g and i). There were insignificant alternations in mRNA expression levels of Atg5, Atg7 as well as Atg16L1 in the $CuSO_4$-treated groups (Fig. 3h, j and k).

Furthermore, mouse-derived spermatogonia cell line GC-1 spg cells were treated with $CuSO_4$ for 12 or 24 h. The results showed that $CuSO_4$ treatment induced autophagy which featured by increasing in the LC3-II/LC3-I ratio and decreasing in p62 protein level (Fig. 4a and b). Meanwhile, the AMPK-mTOR signal pathway proteins including *p*-AMPK, *p*-mTOR were significantly increased (Fig. 4c and d). To confirm the role of AMPK-mTOR signal pathway in $CuSO_4$-induced autophagy in the GC-1 spg cells. AMPK inhibitor (Compound C) was co-treatment with $CuSO_4$. We found that the inhibition of *p*-AMPK by compound C could abolish the induction of autophagy by $CuSO_4$ (Fig. 4f), indicating that AMPK-mTOR signal pathway was involved in $CuSO_4$-induced autophagy of mouse GC-1 spg cells.

3.3. $CuSO_4$ induced autophagy through oxidative stress

Our previous study has demonstrated that $CuSO_4$ treatment can induce oxidative stress in mice testis. Oxidative stress has certain effects during $CuSO_4$-induced apoptosis as well as DNA damage [16]. Nevertheless, it remains unclear if oxidative stress plays a role in the autophagy induced by $CuSO_4$. For determining how oxidative stress affects the $CuSO_4$-induced autophagy, NAC was used for inhibiting the oxidative stress *in vivo* and vitro.

In the vitro study, ROS contents were significantly increased in $CuSO_4$ treatment GC-1 spg cells (Fig. 5a and b). NAC can efficiently suppress the ROS accumulation induced by $CuSO_4$ (Fig. 5c). We found that the inhibition of ROS by NAC could rescue the inhibition of cell viability and the promotion of apoptosis by $CuSO_4$ (Fig. 5d and e). The

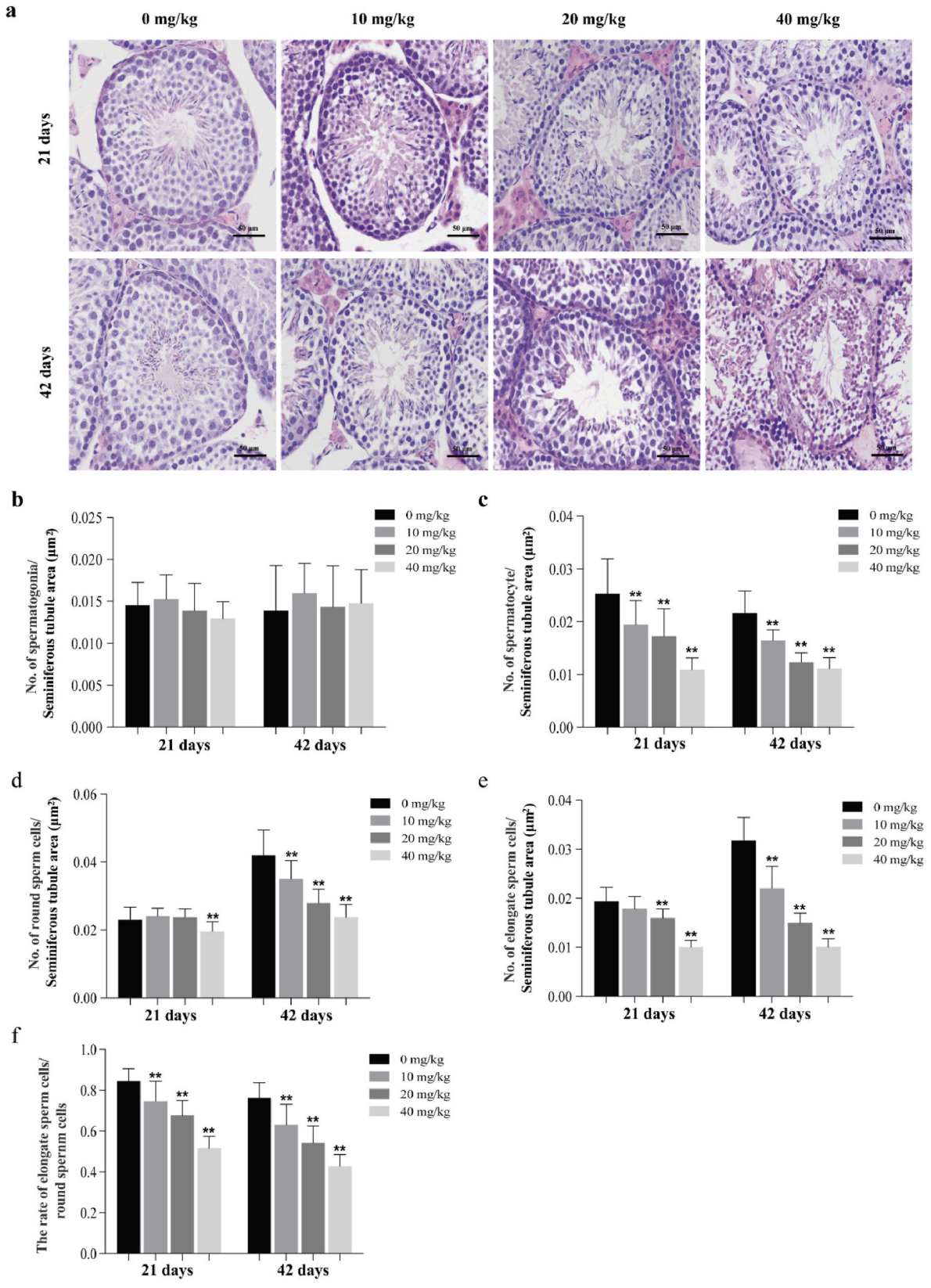

Fig. 1. $CuSO_4$ induces alterations in testicular structure.
(a) Testicular histopathological figures of mice exposed to $CuSO_4$. Histopathological lesions are found in three Cu-treated groups. Spermatogonia and spermatocytes are significantly decreased, and spermatogenic cells show vacuolar degeneration and necrosis. **(b)** The quantification of seminiferous tubule area (μm^2). **(c)** The spermatogonia count. **(d)** The spermatocyte count. **(e)** The round spermatid count **(f)** The elongated spermatid count. **(g)** The ratio of elongated spermatids to round spermatids. Data are presented with the means ± standard deviation. **$p < 0.01$, compared with the control group.

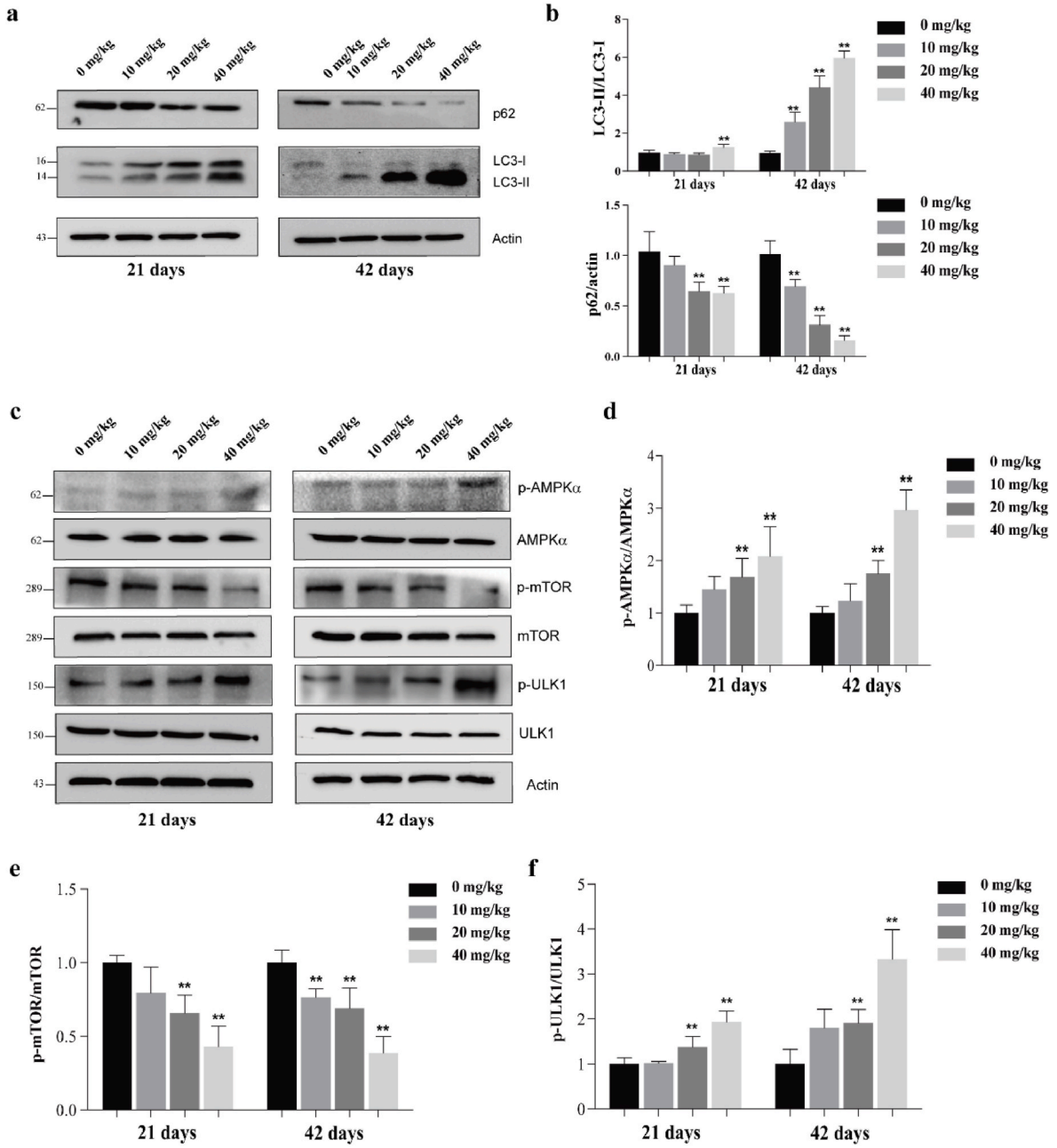

Fig. 2. $CuSO_4$ induces autophagy via AMPK/mTOR pathway in the testis.
(a) The Western blot results of LC3 and p62 protein expression. **(b)** The quantification of LC3-II/LC3-I and p62. **(c)** The Western blot results of *p*-AMPK, AMPK, *p*-mTOR, mTOR, *p*-ULK1 and ULK1 protein expression. **(d)** The quantification of *p*-AMPK/AMPK. **(e)** The quantification of *p*-mTOR/mTOR. **(f)** The quantification of *p*-ULK1/ULK1. Data are presented with the means ± standard deviation. *p < 0.05 and **p < 0.01, compared with the control group.

reduction of ROS could inhibit the autophagy (the reduction of LC3-II/LC3-I ratio) that induced by $CuSO_4$ (Fig. 5f). Furthermore, the AMPK-mTOR pathway, including *p*-AMPK and *p*-mTOR was dramatically reversed by NAC (Fig. 5f).

Similar to the in vitro study, as shown in Fig. 6a, b, c, d and e, the T-AOC activity, SOD activity, CAT activity, GSH-Px activity as well as GSH content had been significantly suppressed in $CuSO_4$-treated group, and, co-treatment with NAC could abolish $CuSO_4$-induced suppression. In the meanwhile, NAC co-treatment could decrease MDA production induced by $CuSO_4$ (Fig. 4f). Also, co-treatment with NAC could abolish the inhibition of CuZn-SOD, Mn-SOD, CAT and GSH-Px mRNA expression levels by $CuSO_4$ (Fig. 6g). Testicular histopathological changes induced by $CuSO_4$ was abolished after a co-treatment with NAC (Fig. 6h). Meanwhile, Fig. 6i illustrated that testicular autophagy was inhibited by co-treatment with $CuSO_4$ and NAC, containing the reduction of LC3-II/LC3-I ratio and the growth of p62 protein expression levels, and *p*-AMPK, *p*-mTOR and *p*-ULK1 was dramatically reversed by NAC (Fig. 6j). The above obtained results indicate that $CuSO_4$-induced testicular autophagy may arise from oxidative stress-mediated AMPK-mTOR signal pathway.

3.4. Autophagy plays the protective role in $CuSO_4$-induced ROS production and apoptosis in GC-1 spg cells

It has reported that the double-edged sword (cytoprotection and cytotoxicity) of autophagy in disease. For investigating the relationship of $CuSO_4$-induced autophagy with cell viability, apoptosis and ROS of GC-1 spg cells, a rescue experiment was carried out with the specific

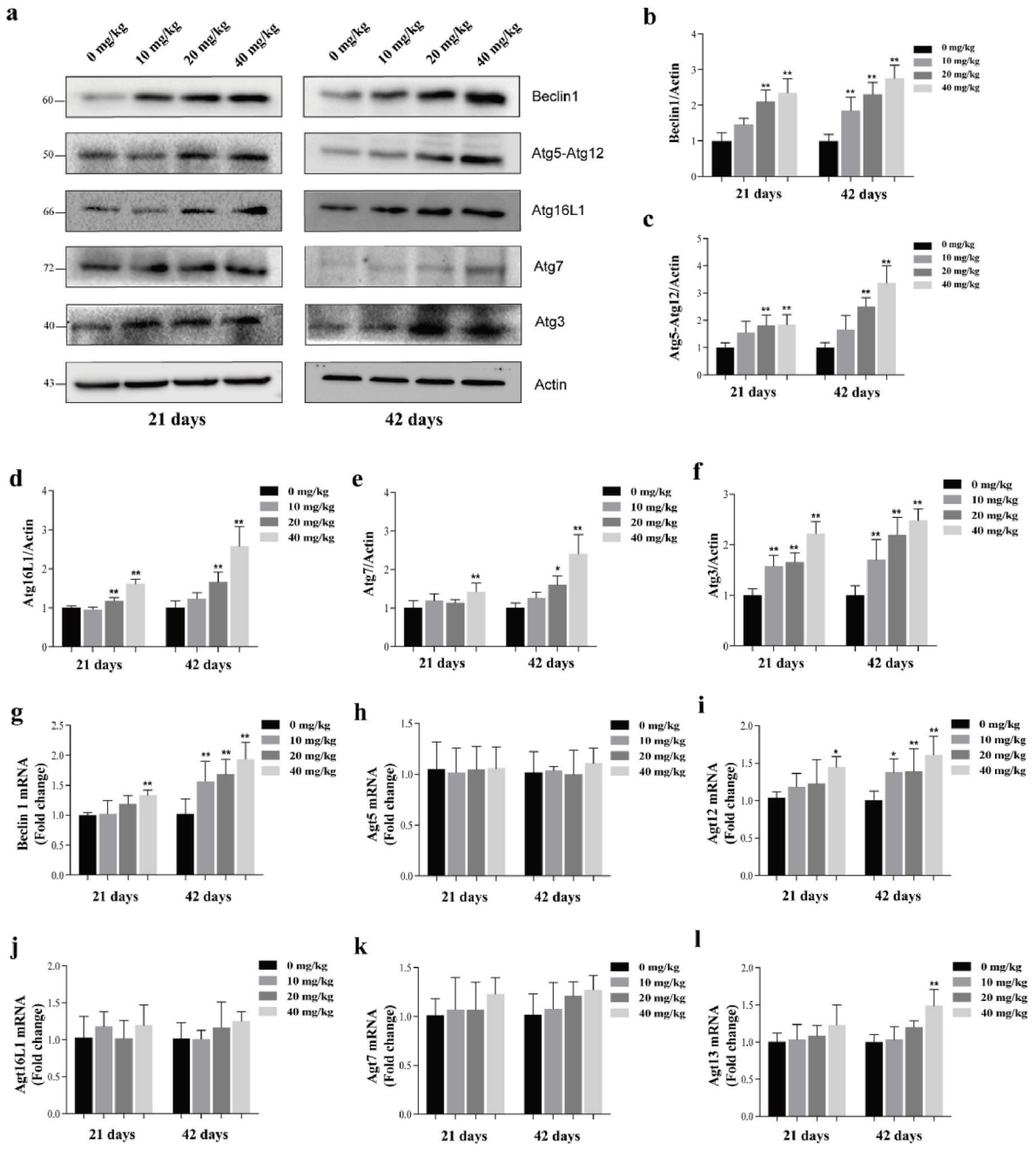

Fig. 3. $CuSO_4$ increases autophagy-related proteins in the testis.
(a) The Western blot results of Beclin1, Atg5-Atg12, Atg16L1, Atg7 and Atg3 protein expression. The quantification of Beclin1 **(b)**, Atg5-Atg12 **(c)**, Atg16L1 **(d)**, Atg7 **(e)** and Atg3 **(f)** protein expression. The mRNA expression of Beclin1 **(g)**, Atg5 **(h)**, Atg12 **(i)**, Atg16L1 **(j)**, Atg7 **(k)** and Atg3 **(l)**. Data are presented with the means ± standard deviation. *p < 0.05 and **p < 0.01, compared with the control group.

autophagy inhibitor 3-MA and Atg5 knock down. The results showed that $CuSO_4$ treatment combined with autophagy inhibition (3-MA or Atg5 knock down) significantly suppressed the expression of LC3-II/LC3-I (Fig. 7a and e). And, down-regulation of cell viability (Fig. 7b and f) and up-regulation of apoptosis (Fig. 7d and h) and ROS production (Fig. 7c and g) were observed in the combination of $CuSO_4$ and autophagy inhibition (3-MA or Atg5 knock down) group when compared with those in $CuSO_4$-treated group. Furthermore, apoptosis inhibition (Z-VAD-FMK) could rescue the inhibition of cell viability by $CuSO_4$ (Fig. 7i and j), but not affect the autophagy (Fig. 7k).

3.5. *Autophagy triggered $CuSO_4$-induced ferroptosis in GC-1 spg cells*

Ferroptosis is a newly defined programmed cell death process with the hallmark of the accumulation of iron-dependent lipid peroxides [25]. It has reported that autophagy also involved in the regulation of ferroptosis [25]. Next, the relationship of $CuSO_4$-induced autophagy with ferroptosis was explored. As shown in Fig. 8a and b, the glutathione eroxidase 4 (GPX4) protein expression levels experienced a significant ($p < 0.05$ or < 0.01) increase and cyclooxygenase 2 (COX-2) protein expression levels were significantly ($p < 0.05$ or < 0.01) decreased in the $CuSO_4$-treated cells. GPX4 and COX-2 are the marker of ferroptosis. Above results indicated that $CuSO_4$ could induce ferroptosis in the GC-1 spg cells. And, co-treatment with autophagy inhibition (3-MA or Atg5

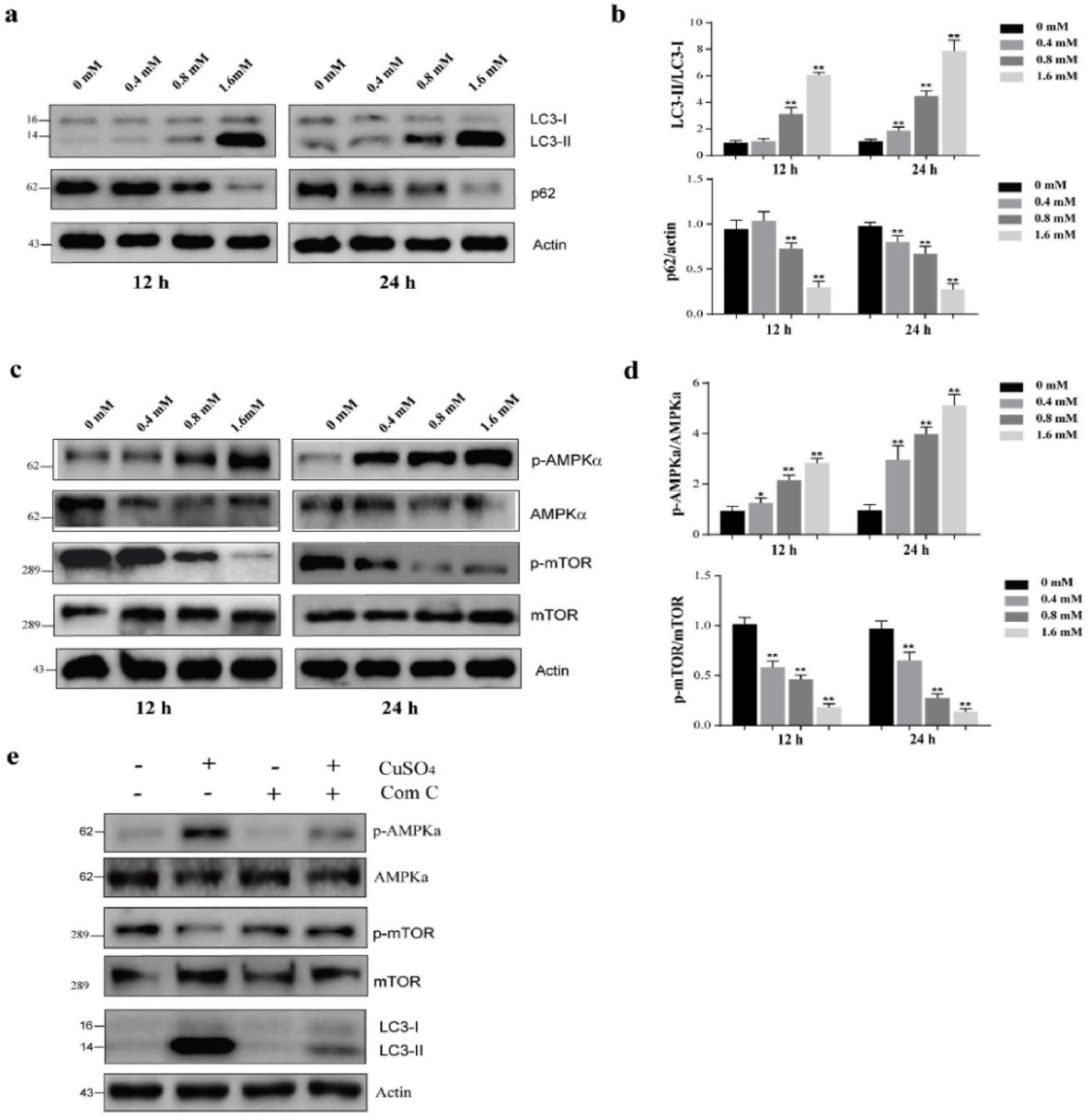

Fig. 4. $CuSO_4$ induces autophagy via AMPK/mTOR pathway in the GC-1 spg cells.
(a) Cells were treated with $CuSO_4$ (0, 0.4, 0.8 and 1.6 mM) for 12h and 24h. The Western blot results of LC3 and p62 protein expression. **(b)** The quantification of LC3-II/LC3-I and p62. **(c)** Cells were treated with $CuSO_4$ (0, 0.4, 0.8 and 1.6 mM) for 12h and 24h. The Western blot results of *p*-AMPKα, AMPKα, *p*-mTOR and mTOR protein expression. **(d)** The quantification of *p*-AMPKα/AMPKα and *p*-mTOR/mTOR. **(e)** Cells were treated with $CuSO_4$ (1.6 mM, 24h) in the presence/absence of Compound C (20 μM, 4h). The Western blot results of *p*-AMPK, AMPK, *p*-mTOR, mTOR and LC3 protein expression. Data are presented with the means ± standard deviation. *$p < 0.05$ and **$p < 0.01$, compared with the control group.

knock down) could rescue the induction of ferroptosis by $CuSO_4$ (Fig. 8c and d), indicating that autophagy triggered ferroptosis. Meanwhile, in comparison with $CuSO_4$ treatment group, protein expression levels in nuclear receptor coactivator 4 (NCOA4) and ferritin heavy chain 1 (FTH1) were increased in the $CuSO_4$ group co-treatment with autophagy inhibition (3-MA or Atg5 knock down) group (Fig. 8c and d), indicating that autophagy triggered ferroptosis through degradation of ferritin.

3.6. Autophagy protected the $CuSO_4$-induced spermatogenesis disorder in the testis

The vitro study showed the protection role of autophagy. Next, the role of autophagy was verified in the mice. Fig. 9a demonstrated that autophagy was significantly inhibited by co-treatment with $CuSO_4$ and 3-MA group. Testicular histopathological changes showed greater severity in the 3-MA+$CuSO_4$ group in comparison with the $CuSO_4$-treated group (Fig. 9b). Besides, the sperm motility (Fig. 9c) and sperm concentrations (Fig. 9d) in the 3-MA+$CuSO_4$ group were remarkably inferior ($p < 0.01$) to those in the $CuSO_4$-treated group. The above findings indicated that autophagy played the protective role in $CuSO_4$-induced testicular damage and spermatogenesis disorder.

As shown in Fig. 10a, T-AOC activity, SOD activity, CAT activity, GSH-Px activity as well as GSH content in the 3-MA+$CuSO_4$ group remarkably reduced in comparison with the $CuSO_4$-treated group, and, MDA content was increased. Meanwhile, mRNA expression levels in CuZn-SOD, Mn-SOD, CAT and GSH-Px seemed lower compared with those in the $CuSO_4$-treated group (Fig. 10b). Based on these findings, autophagy exerted the protective role in $CuSO_4$-induced testicular oxidative damage. Former research proves that $CuSO_4$ treatment induces apoptosis in mouse testis [16]. Subsequently, we explored

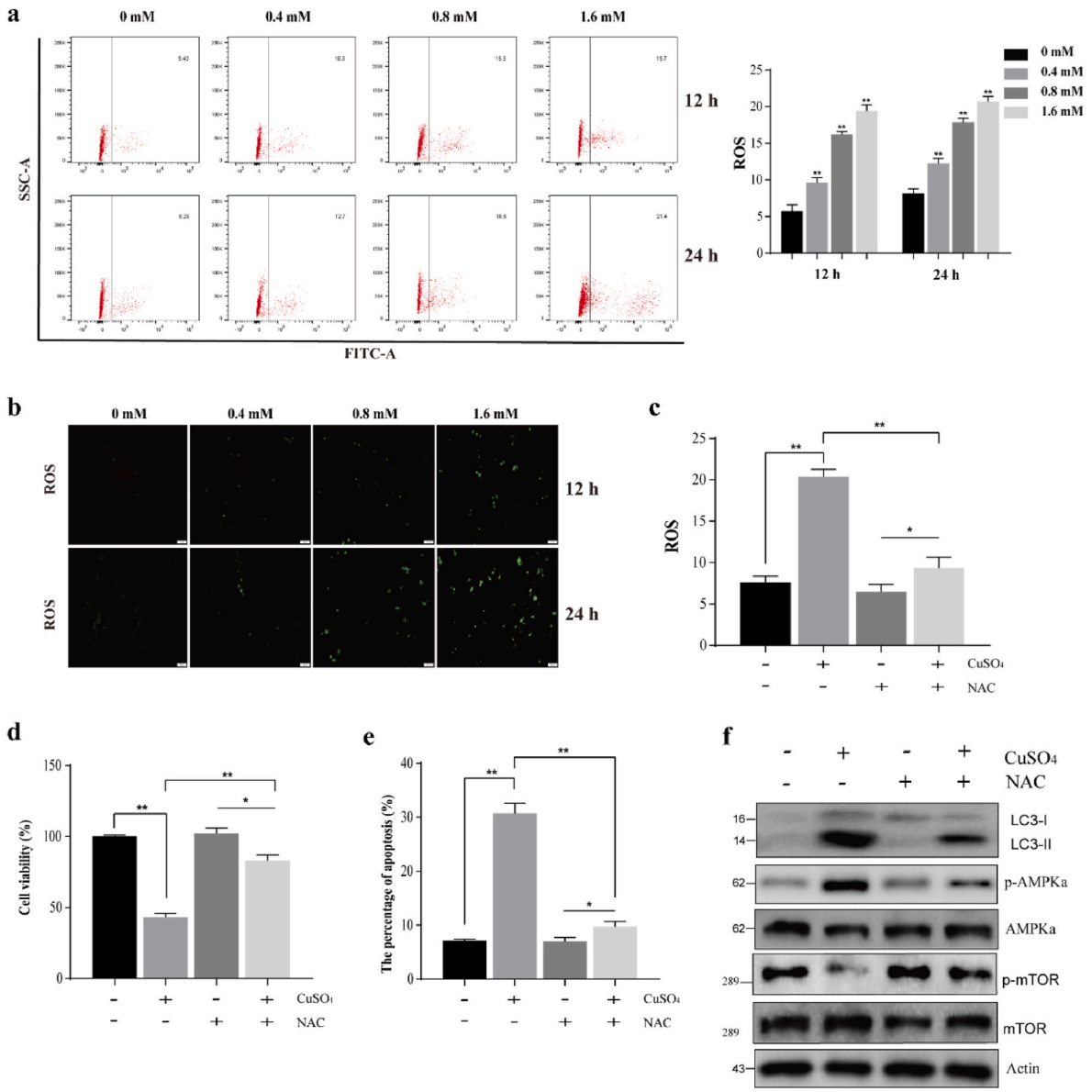

Fig. 5. $CuSO_4$ induces autophagy through ROS in the GC-1 spg cells.
Cells were treated with $CuSO_4$ (0, 0.4, 0.8 and 1.6 mM) for 12h and 24h. Relative ROS amounts determined by flow cytometry **(a),** relative ROS amounts determined by DCFH-DA staining of CuSO4-primed RAW264.7 cells **(b)**. Cells were treated with $CuSO_4$ (1.6 mM, 24h) in the presence/absence of NAC (5 mM, 24h), relative ROS amounts determined by flow cytometry **(c),** the changes of ROS **(d)** and apoptosis **(e)**, the Western blot results of *p*-AMPK, AMPK, *p*-mTOR, mTOR and LC3 protein expression **(f)**. Data are presented with the means ± standard deviation. *p < 0.05 **p < 0.01.

whether autophagy played the protection role through apoptosis in the testis. In comparison with $CuSO_4$ treatment group, protein expression levels in apoptosis-linked proteins such as cleaved-caspase-3, cleaved-caspase-8, cleaved-caspase-9, cleaved-PARP and caspase-12 were increased in the 3-MA+$CuSO_4$ group (Fig. 10c). Besides, similar to the vitro experiment results, Fig. 10d illustrated the co-treatment with $CuSO_4$ and Z-VAD-FMK could suppress apoptosis induced by $CuSO_4$, however, it was not affect the autophagy. Testicular histopathological changes could be eradicated in part in the Z-VAD-FMK+$CuSO_4$ group in comparison with the $CuSO_4$-treated group (Fig. 10e). And, the sperm motility (Fig. 10f) and sperm concentrations (Fig. 10g) in the Z-VAD-FMK +$CuSO_4$ group were remarkably greater ($p < 0.05$ or $p < 0.01$) compared with those in the $CuSO_4$-treated group. These results indicated that autophagy played protective role through inhibition of oxidative damage and apoptosis.

Otherwise, in the testis, the results also showed that $CuSO_4$ treatment induce ferroptosis, which featured by decrease in GPX4 and increase in COX-2 (Fig. 11a and b). And, the iron concentration in the testis was significantly increased in the $CuSO_4$-treated mice (Fig. 11c). Similar to the vitro experiment results, Fig. 11d illustrated the co-treatment with $CuSO_4$ and 3-MA could suppress ferroptosis induced by $CuSO_4$. This results indicated that autophagy also played adverse role through promotion of ferroptosis.

4. Discussion

Cu is an important trace element for human and animals at low concentration, whereas, over-exposure to Cu has detrimental influences. At present, the environmental pollution is the important resource of overexposure to copper. Otherwise, dis-regulated copper levels can be also discovered from many metabolic and neurodegenerative illnesses [26]. Recent studies have demonstrated that the male fertility is also the target of Cu toxicology, however, the precise mechanism is still unclear.

Our previous study have proved that Cu can accumulated into the

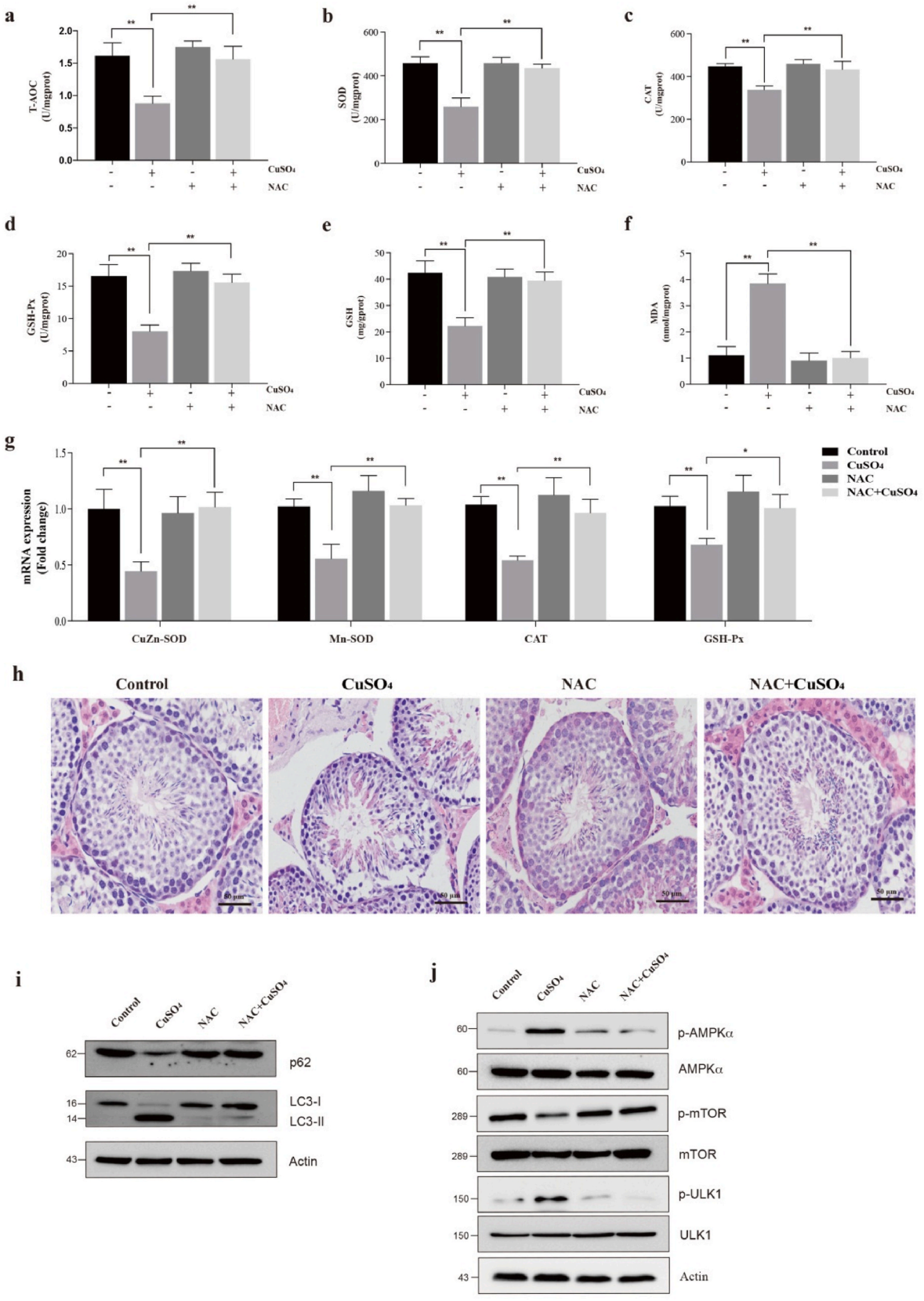

Fig. 6. Oxidative stress is the inductor of $CuSO_4$-induced autophagy in the testis.
The changes of T-AOC activity **(a)**, SOD activity **(b)**, CAT activity **(c)**, GSH-Px activity **(d)**, GSH content **(e)**, MDA content **(f)**, and the changes of CuZn-SOD, Mn-SOD, CAT and GSH-Px mRNA expression **(g)** after co-treatment with NAC and $CuSO_4$. **(h)** The histopathological lesions after co-treatment with NAC and $CuSO_4$. **(i)** The Western blot results of LC3 and p62 in the testis after co-treatment with NAC and $CuSO_4$. **(j)** The Western blot results of *p*-AMPK, AMPK, *p*-mTOR, mTOR, *p*-ULK1 and ULK1 after co-treatment with NAC and $CuSO_4$. Data are presented with the means ± standard deviation. *p < 0.05 **p < 0.01.

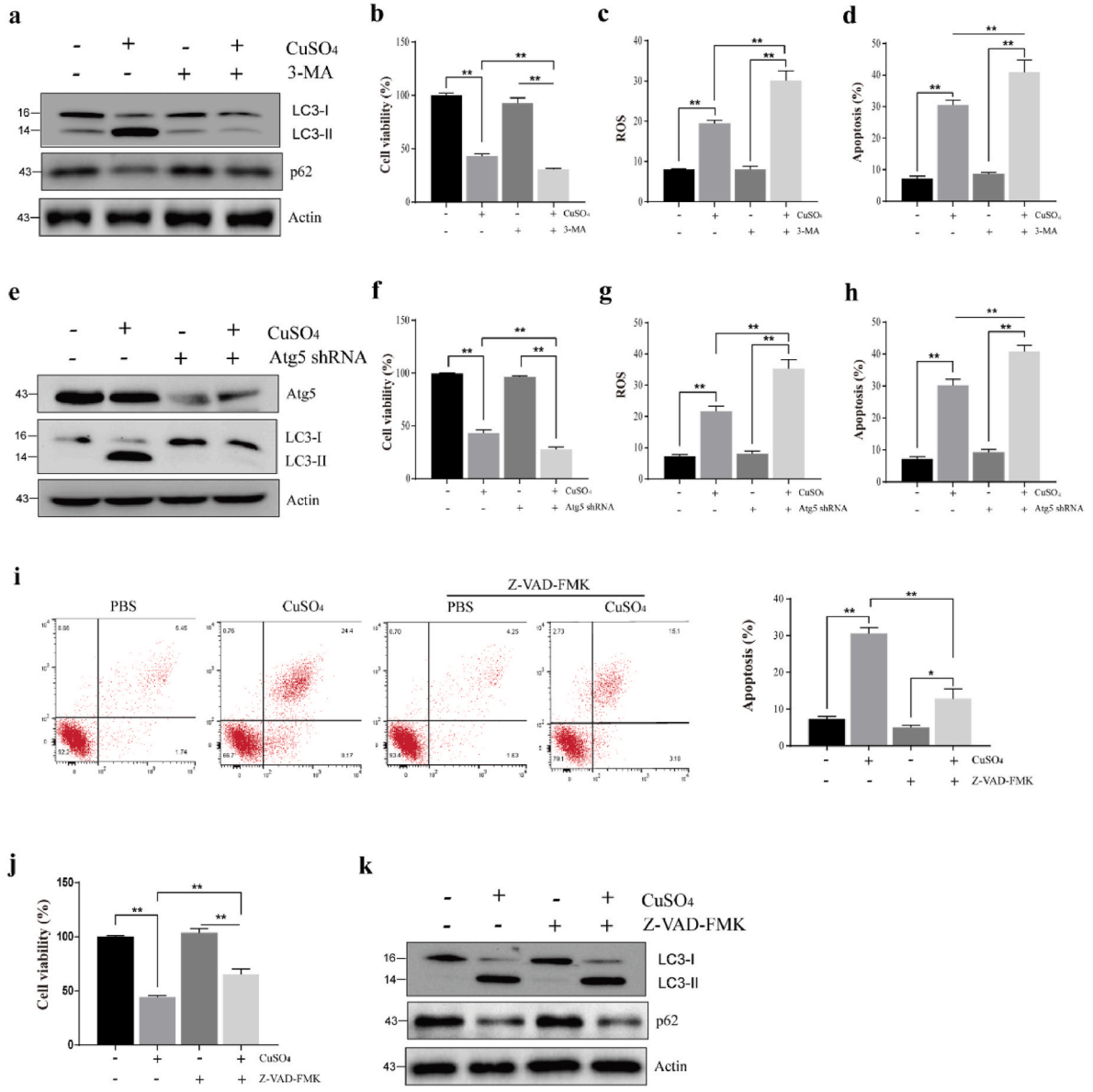

Fig. 7. Autophagy plays the protective role in $CuSO_4$-induced ROS production and apoptosis in GC-1 spg cells.
Cells were treated with $CuSO_4$ (1.6 mM, 24h) in the presence/absence of 3-MA (1 mM, 1h), the changes of autophagy **(a)**, cell viability **(b)**, the ROS amounts **(c),** and the percentage of apoptosis in GC-1 spg cells **(d)**. Cells transfected with control shRNA and ATG5 shRNA exposed with $CuSO_4$ (1.6 mM) for 24 h, changes of autophagy **(e)**, cell viability **(f)**, the ROS amounts **(g),** and the percentage of apoptosis in GC-1 spg cells **(h)**. Cells were treated with $CuSO_4$ (1.6 mM, 24h) in the presence/absence of Z-VAD-FMK (20 μM, 1h), the changes of the percentage of apoptosis **(i)**, and autophagy **(j)**. Data are presented with the means ± standard deviation. *$p < 0.05$ **$p < 0.01$.

testis [27], which consistent with other studies [28]. Cu is absorbed from the intestines of animals, and then transported into the blood, and then accumulated in tissues and organs as blood circulates. During this process, copper transporter (Ctr) family, p-type ATPase and copper chaperones also play key roles in copper absorption, transport and homeostasis [29–31]. However, the specific mechanism of copper accumulation in testis has not been studied. It has been also reported that over-exposure Cu can induce testicular damage and decrease serum testosterone production [32,33]. Our previous study has demonstrated excessive exposure to Cu induces reproductive toxicity, such as the decrease of sperm concentration and sperm motility, and growth of sperm malformation rate [16]. In the present study, germ cell counting and histopathological analysis showed a decrease in the number of spermatocytes, round spermatids and elongated spermatids.

Despite that there are many studies concerning Cu-related testicular toxicology, few of them concentrate on the mechanism of testicular toxicology about Cu. Autophagy, a form of cell decomposition, has certain associations with the transfer of material from cytoplasm to lysosomes [17]. Autophagy is reported to be involved in various diseases and heavy metals toxicology. Recent studies have shown that uncontrolled or overstimulated autophagy may intermediate cell death. Reports prove that Cu can serve as one new autophagy stimulator [34,35]. Whereas, it is still unknown if autophagy is related to Cu reproduction toxicity. In the current study, $CuSO_4$ treatment increased LC3-II/LC3–I ratio and reduced p62 protein expression, indicating the role of $CuSO_4$ in inducing testicular autophagy in mice. Meanwhile, $CuSO_4$ could increase autophagy levels in mouse-derived spermatogonia cell line GC-1 spg cells. In consistence with previous findings, Shao et al. [36] have reported that $CuSO_4$ exposure can induce autophagy in the chicken testis. Additionally, the obtained results from Kang et al. [37] also prove Cu compounds lead to an increase of autophagy in male germ cells.

Next, the potential mechanism of autophagy induced by $CuSO_4$ was

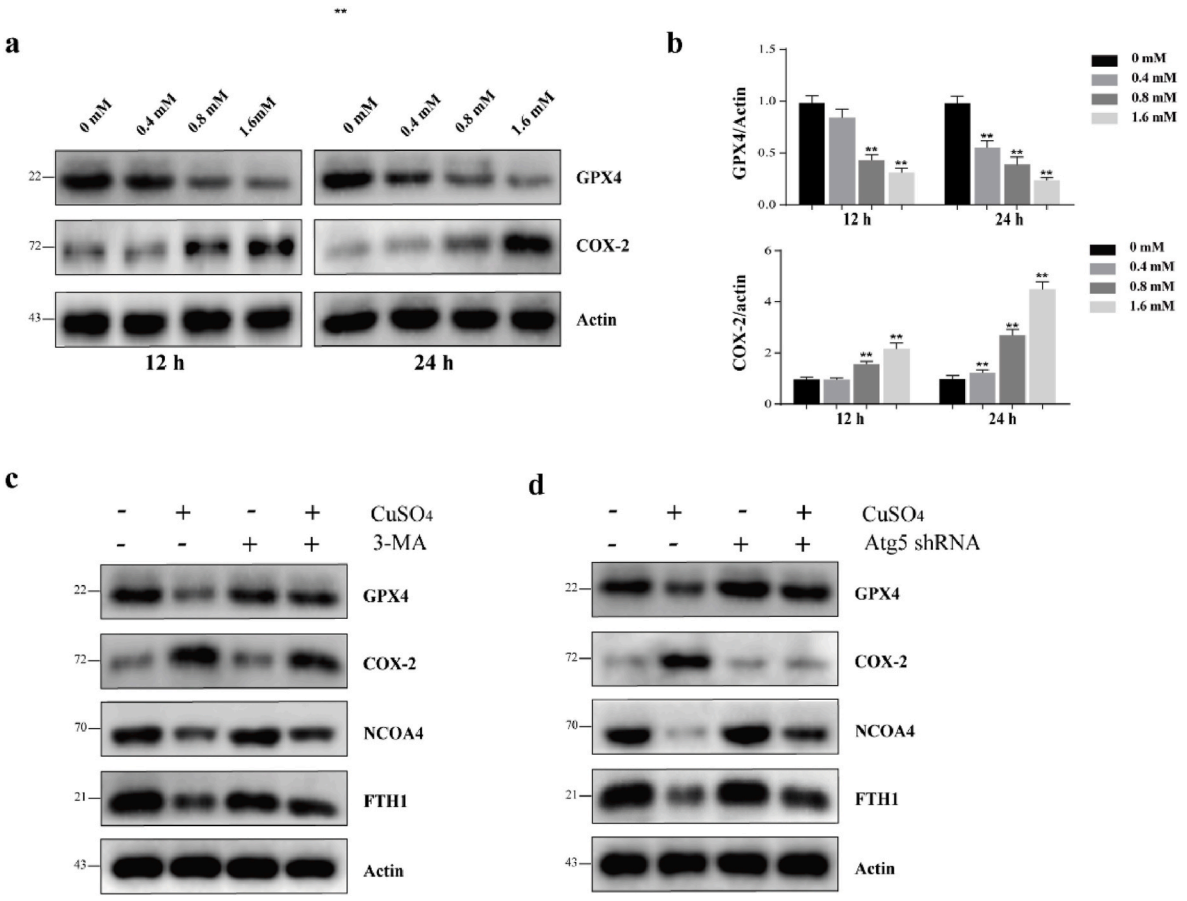

Fig. 8. Autophagy triggered ferroptosis in $CuSO_4$-treated GC-1 spg cells.
(a) Cells were treated with $CuSO_4$ (0, 0.4, 0.8 and 1.6 mM) for 12h and 24h. The Western blot results of GPX4 and COX-2 protein expression. **(b)** The quantification of GPX4 and COX-2. **(c)** Cells were treated with $CuSO_4$ (1.6 mM, 24h) in the presence/absence of 3-MA (1 mM, 1h), the changes of GPX4, COX-2, NCOA4 and FTH1. **(d)** Cells transfected with control shRNA and ATG5 shRNA exposed with $CuSO_4$ (1.6 mM) for 24 h, changes of GPX4, COX-2, NCOA4 and FTH1. Data are presented with the means ± standard deviation. *p < 0.05 **p < 0.01.

explored. AMPK-mTOR pathway is an important signaling pathway in autophagy. Autophagy, driven by AMPK, can serve as one crucial sensor to regulate cellular metabolism, and maintain energy homeostasis. AMPK activation possibly results in autophagy by mTOR negative regulation. Additionally, AMPK straightforwardly phosphorylates ULK1 to trigger autophagy. The increase in *p*-AMPK and *p*-ULK1 and decrease in *p*-mTOR reveal that $CuSO_4$ activates AMPK-mTOR pathway in the testis and GC-1 spg cells. Meanwhile the AMPK inhibiter experiment was confirmed that $CuSO_4$ induced autophagy through the AMPK-mTOR pathway. Similar to our results, the results of Liao et al. [38] prove the facilitating role of Cu in autophagy through AMPK-mTOR pathway in chicken kidney. In the meantime, proteins related to autophagy flux had been also observed by the current research. Beclin1, a major gene promoting initiate autophagy, gets engaged in the initiation stage of autophagy. The Atg12-Atg5-Atg16L1 complex seems indispensable to autophagosome formation and makes for phagophore expansion. LC3-I is activated by Atg 7 and conjugated to phosphatidylethanolamine by Atg 3 to form LC3-II, which is referred to as LC3 lipidation. Furthermore, the Atg 12- Atg 3 complex plays a crucial part in basic autophagy flux, endosome function as well as endolysosomal transport during the late nuclear period. According to the results in the present study, Beclin1, Atg5-Atg12, Atg7 Atg3 as well as Atg16L1 all increased in the testis after $CuSO_4$ treatment. Consistent with our results, $CuSO_4$ treatment increases Beclin-1, Atg 7, Atg 5, Atg 3 expressions in the renal tubular epithelial cells of ducks [39]. In addition, Li et al. [20] has indicated that 250 mg/kg Cu treatment can increase mRNA and protein expression levels in Beclin1 and Atg 5 in the myocardium of pigs.

Research shows that oxidative damage is important to the testicular damage induced by $CuSO_4$ [40,41]. Our previous study has demonstrated that $CuSO_4$ treatment can induce ROS in mice testis, and ROS exerts significant effects in the apoptosis and DNA damage induced by $CuSO_4$ [16]. It is not known whether ROS is important to $CuSO_4$-induced autophagy. For demonstrating the effects of oxidative stress on autophagy, oxidative stress inhibitor NAC had co-treatment with $CuSO_4$ to check autophagy changes. As indicated by above findings, treatment with NAC could greatly inhibit the growth of $CuSO_4$-induced autophagy in mouse testis and GC-1 spg cells. Moreover, NAC-co-treatment removed the impacts of $CuSO_4$ treatment on the AMPK-mTOR signaling pathway.

Autophagy can serve as a double-edged sword to regulate cellular death and survival. Autophagy level seems relatively lower in physiological conditions, which is conducive to the survival of cells. Subject to specific chemicals, autophagy may be remarkably activated, leading to the death of cells. For investigating the role of autophagy in testicular damage and spermatogenesis disorder induced by $CuSO_4$, autophagy inhibitor (3-MA) and Atg5 knock down were used. The results illustrated that autophagy inhibition aggravated the testicular damage and spermatogenesis disorder induced by $CuSO_4$, indicating that autophagy played protective role in $CuSO_4$-induced spermatogenesis disorder. Also, Yang et al. [42] has reported that autophagy may attenuate Cu-induced mitochondrial dysfunction. It has been confirmed that autophagy can inhibit cell death through against apoptosis. To further identify the protective mechanism of autophagy in $CuSO_4$-induced spermatogenesis disorder, as a double-edged sword, a rescue experiment needed to be

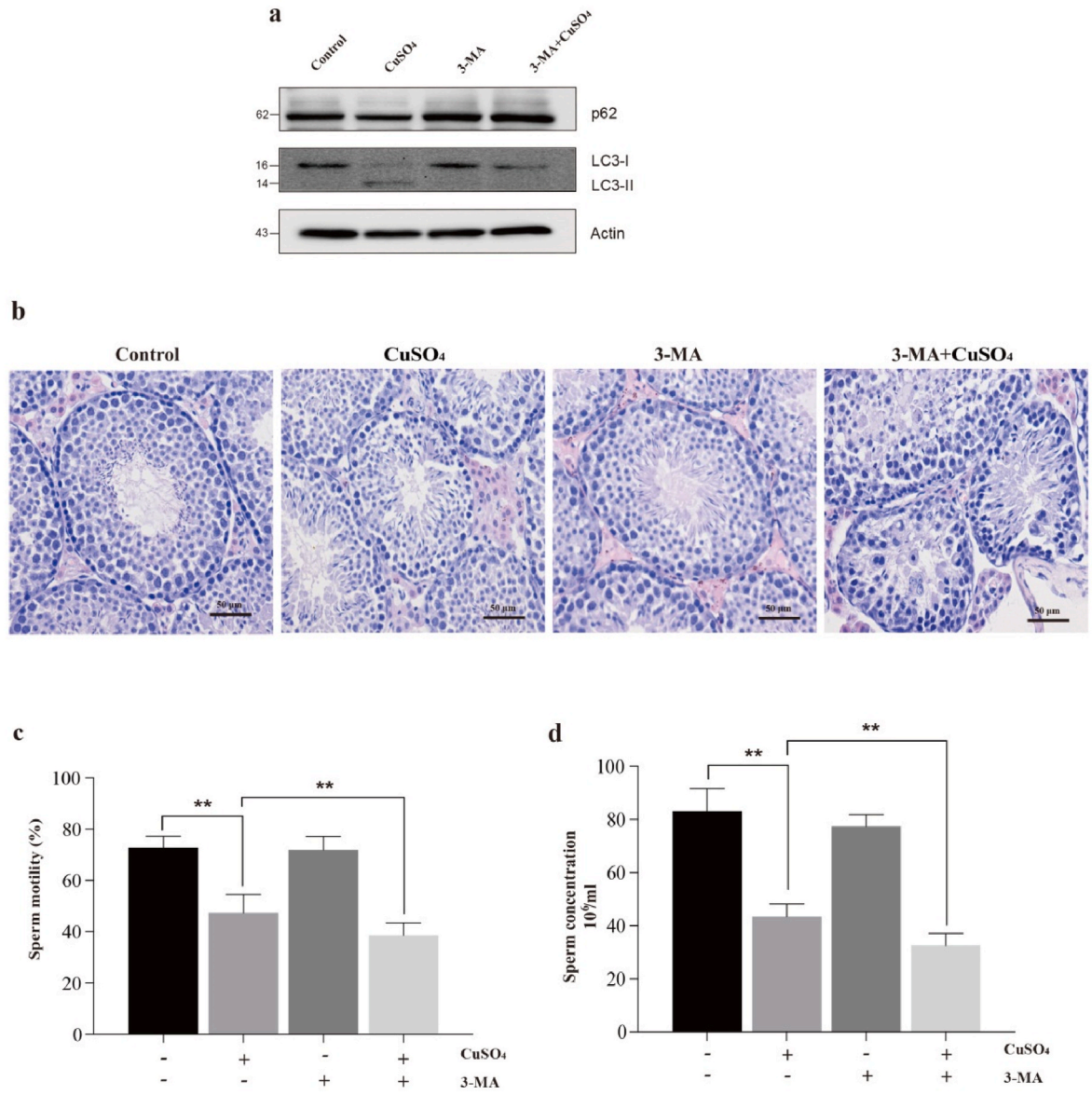

Fig. 9. Autophagy plays the protective role in $CuSO_4$-induced spermatogenesis disorder in the testis.
(a) The Western blot results of LC3 and p62 after co-treatment with autophagy inhibitor (3-MA) and $CuSO_4$. **(b)** The histopathological lesions after co-treatment with autophagy inhibitor (3-MA) and $CuSO_4$. **(c)** The sperm motility changes after co-treatment with autophagy inhibitor (3-MA) and $CuSO_4$. **(d)** The sperm concentration changes after co-treatment with autophagy inhibitor (3-MA) and $CuSO_4$. Data are presented with the means ± standard deviation. *p < 0.05, **p < 0.01.

performed with the given autophagy inhibitor (3-MA) or Atg5 knock down to inhibit the autophagy induced by $CuSO_4$. Indeed, the oxidative damage (or ROS production) and apoptosis were increased when being co-treated with 3-MA or Atg5 knock down and $CuSO_4$ in this work. Consistent with the results in our former research, Wu et al. [43] have illustrated the role of inhibited autophagy in enhancing apoptosis induced by $CuSO_4$ in non-small cell lung cancers. Furthermore, co-treatment apoptosis inhibitor (Z-VAD-FMK) with $CuSO_4$ could dramatically partly abolish $CuSO_4$-induced testicular damage and spermatogenesis disorder, which suggested that autophagy played protective role through inhibition of apoptosis. Recently studies have demonstrated that autophagy also involve in the regulation of ferroptosis, which is a non-apoptotic form of cell death [44]. Next, we explored whether ferroptosis was involved in $CuSO_4$-induced testicular damage and spermatogenesis disorder, and its relationship with autophagy. Indeed, the results showed that $CuSO_4$ treatment could induce ferroptosis in *vitro* and *vivo*, which was associated with the up-regulation of COX-2 and down-regulation of GPX-4. Moreover, autophagy inhibition could suppress the ferroptosis induced by $CuSO_4$, indicating that autophagy promote ferroptosis in this study. Several studies have reported that activation of the autophagy pathway promotes ferroptosis by degradation of ferritin [45]. FTH1 is an important ferritin and is a regulatory factor in iron metabolism [44]. NCOA4 is a selective cargo receptor for the autophagic turnover of ferritin [25]. Our results showed that $CuSO_4$ can decrease FTH1 and NCOA4 protein expression, however, co-treatment autophagy inhibition could rescue the reduction of FTH1 and NCOA4, indicating that autophagy triggered ferroptosis through degradation of ferritin.

Altogether, abovementioned results indicated that $CuSO_4$ induced autophagy via oxidative stress-dependent AMPK-mTOR pathway in the GC-1 cells and testis, and autophagy play activation possibly led to the generation of protection mechanism through oxidative damage and apoptosis inhibition, however, autophagy also aggravate $CuSO_4$ toxicology through promoting ferroptosis. Overall, autophagy plays a positive role for attenuating $CuSO_4$-induced testicular damage and spermatogenesis disorder. Our study provides a possible targeted

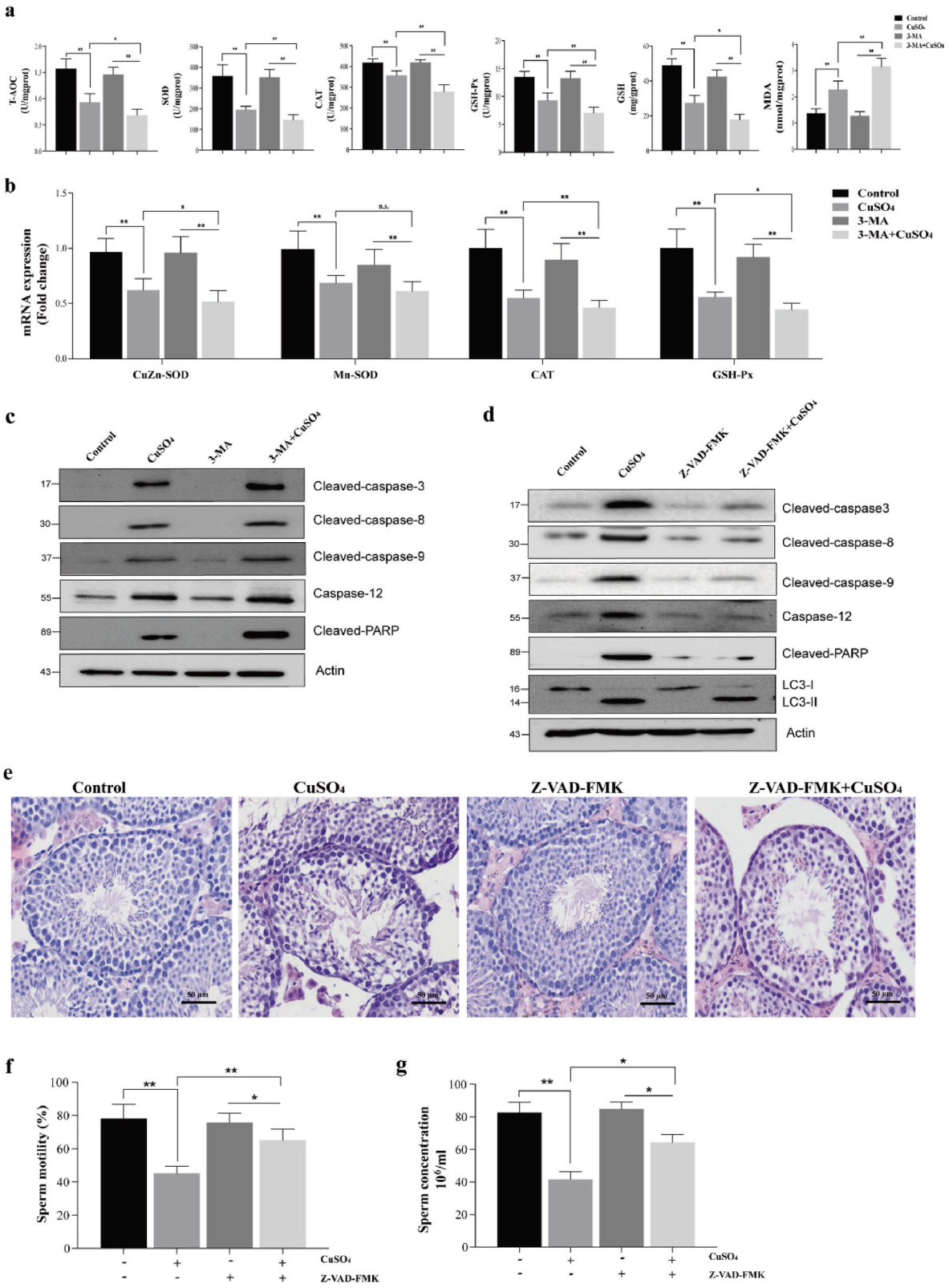

Fig. 10. Autophagy inhibits $CuSO_4$-induced oxidative stress and apoptosis in the testis.
(a) The changes of T-AOC activity, SOD activity, CAT activity, GSH-Px activity, GSH content, and MDA content after co-treatment with 3-MA and $CuSO_4$. **(b)** The changes of CuZn-SOD, Mn-SOD, CAT and GSH-Px mRNA expression after co-treatment with 3-MA and $CuSO_4$. **(c)** The Western blot results of cleaved-caspase-3, cleaved-caspase-8, cleaved-caspase-9, caspase-12 and cleaved-PARP after co-treatment with autophagy inhibitor (3-MA) and $CuSO_4$. **(d)** The Western blot results of cleaved-caspase-3, cleaved-caspase-8, cleaved-caspase-9, caspase-12, cleaved-PARP and LC3 after co-treatment with apoptosis inhibitor (Z-VAD-FMK) and $CuSO_4$. **(e)** The histopathological lesions after co-treatment with apoptosis inhibitor (Z-VAD-FMK) and $CuSO_4$. **(f)** The sperm motility changes after co-treatment with apoptosis inhibitor (Z-VAD-FMK) and $CuSO_4$. **(g)** The sperm concentration changes after co-treatment with apoptosis inhibitor (Z-VAD-FMK) and $CuSO_4$. Data are presented with the means ± standard deviation. *$p < 0.05$, **$p < 0.01$.

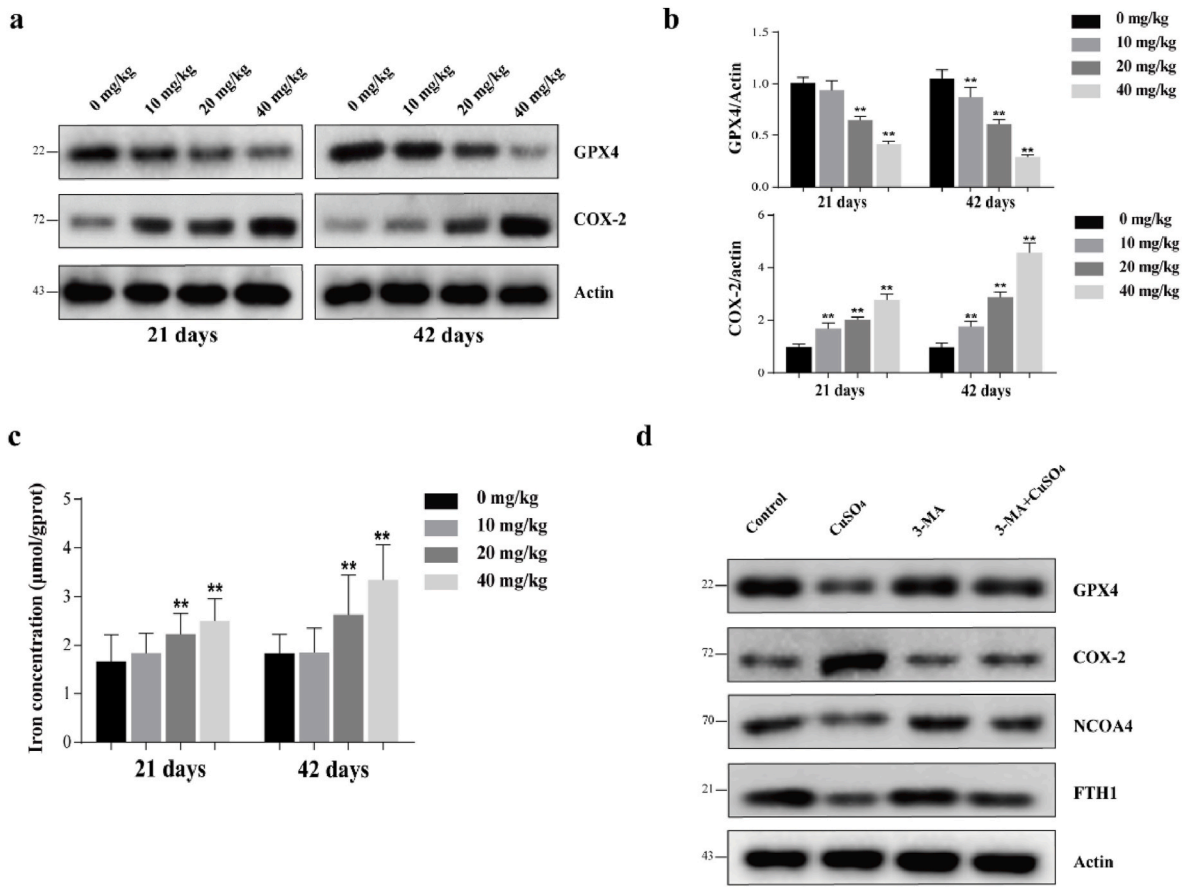

Fig. 11. Autophagy promoted $CuSO_4$-induced ferroptosis in the testis.
(a) The Western blot results of GPX4 and COX-2 protein expression. **(b)** The quantification of GPX4 and COX-2. **(c)** The content of iron concentration in the testis. (d) The Western blot results of GPX4, COX-2, NCOA4 and FTH1 after co-treatment with autophagy inhibitor (3-MA) and $CuSO_4$. Data are presented with the means ± standard deviation. *p < 0.05 **p < 0.01.

therapy for Cu overload-induced reproduction toxicology.

Credit authors contribution statement

Hongrui Guo: Conceptualization, Experiment design, Writing - review & editing, Funding acquisition. Yujuan Ouyang: Experimental section, Data analysis, Writing - original draft. Heng Yin: Experimental section, Data analysis, Writing - original draft. Hengmin Cui: Conceptualization, Experiment design, Writing - review & editing, Funding acquisition. Huidan Deng: Conceptualization, Experiment design, Writing - review & editing, Funding acquisition. Huan Liu: Experimental section, Data analysis. Zhijie Jian: Experimental section, Data analysis. Jing Fang: Writing - review & editing. Zhicai Zuo: Writing - review & editing. Xun Wang: Writing - review & editing. Ling Zhao: Writing - review & editing. Yanqiu Zhu: Writing - review & editing. Yi Geng: Writing - review & editing. Ping Ouyang: Writing - review & editing.

Data availability statement

The data that support the findings of this study are available from the corresponding author upon reasonable request.

Declaration of competing interest

The authors declare that they have no known competing financial interests or personal relationships that could have appeared to influence the work reported in this paper.

Acknowledgments

The study was supported by Sichuan Science and Technology Program (2020YJ0113), the program for Changjiang scholars and the university innovative research team (IRT 0848), and the Shuangzhi project of Sichuan Agricultural University (03573050; 2021993249).

References

[1] C. Cadenas, Highlight report: toxicology of copper, Arch. Toxicol. 89 (12) (2015) 2471–2472.
[2] Z. Shabbir, A. Sardar, A. Shabbir, G. Abbas, S. Shamshad, S. Khalid, Natasha, G. Murtaza, C. Dumat, M. Shahid, Copper uptake, essentiality, toxicity, detoxification and risk assessment in soil-plant environment, Chemosphere 259 (2020), 127436.
[3] H. Guo, Z. Jian, H. Liu, H. Cui, H. Deng, J. Fang, Z. Zuo, X. Wang, L. Zhao, Y. Geng, P. Ouyang, H. Tang, TGF-β1-induced EMT activation via both Smad-dependent and MAPK signaling pathways in Cu-induced pulmonary fibrosis, Toxicol. Appl. Pharmacol. 418 (2021), 115500.
[4] H. Guo, Y. Wang, H. Cui, Y. Ouyang, T. Yang, C. Liu, X. Liu, Y. Zhu, H. Deng, Copper induces spleen damage through modulation of oxidative stress, apoptosis, DNA damage, and inflammation, Biol. Trace Elem. Res. (2021), https://doi.org/10.1007/s12011-021-02672-8.
[5] H. Liu, H. Guo, Z. Jian, H. Cui, J. Fang, Z. Zuo, J. Deng, Y. Li, X. Wang, L. Zhao, Copper induces oxidative stress and apoptosis in the mouse liver, Oxid. Med. Cell. Longev. (2020), 1359164, https://doi.org/10.1155/2020/1359164.
[6] M. Rehman, L. Liu, Q. Wang, M.H. Saleem, S. Bashir, S. Ullah, D. Peng, Copper environmental toxicology, recent advances, and future outlook: a review, Environ. Sci. Pollut. Res. Int. 26 (18) (2019) 18003–18016.
[7] H. Liu, H. Guo, H. Deng, H. Cui, J. Fang, Z. Zuo, J. Deng, Y. Li, X. Wang, L. Zhao, Copper induces hepatic inflammatory responses by activation of MAPKs and NF-κB signalling pathways in the mouse, Ecotoxicol. Environ. Saf. 201 (2020), 110806.
[8] H. Wu, H. Guo, H. Liu, H. Cui, J. Fang, Z. Zuo, J. Deng, Y. Li, X. Wang, L. Zhao, Copper sulfate-induced endoplasmic reticulum stress promotes hepatic apoptosis

by activating CHOP, JNK and caspase-12 signaling pathways, Ecotoxicol. Environ. Saf. 191 (2020), 110236.
[9] Z. Jian, H. Guo, H. Liu, H. Cui, J. Fang, Z. Zuo, J. Deng, Y. Li, X. Wang, L. Zhao, Oxidative stress, apoptosis and inflammatory responses involved in copper-induced pulmonary toxicity in mice, Aging (Albany NY) 12 (17) (2020) 16867–16886.
[10] Y.X. Wang, P. Wang, W. Feng, C. Liu, P. Yang, Y.J. Chen, L. Sun, Y. Sun, J. Yue, L. J. Gu, Q. Zeng, W.Q. Lu, Relationships between seminal plasma metals/metalloids and semen quality, sperm apoptosis and DNA integrity, Environ. Pollut. 224 (2017) 224–234.
[11] A. Kasperczyk, M. Dobrakowski, Z.P. Czuba, L. Kapka-Skrzypczak, S. Kasperczyk, Environmental exposure to zinc and copper influences sperm quality in fertile males, Ann. Agric. Environ. Med. 23 (1) (2016) 138–143.
[12] Y. Li, Q. Gao, M. Li, M. Li, X. Gao, Cadmium, chromium, and copper concentration plus semen-quality in environmental pollution site, China, Iran. J. Public Health 43 (1) (2014) 35–41.
[13] S. Roychoudhury, P. Massanyi, In vitro copper inhibition of the rabbit spermatozoa motility, J. Environ. Sci. Health A Tox Hazard. Subst. Environ. Eng. 43 (6) (2008) 651–656.
[14] S. Roychoudhury, P. Massanyi, J. Bulla, M.D. Choudhury, L. Straka, N. Lukac, G. Formicki, M. Dankova, L. Bardos, In vitro copper toxicity on rabbit spermatozoa motility, morphology and cell membrane integrity, J. Environ. Sci. Health A Tox Hazard. Subst. Environ. Eng. 45 (12) (2010) 1482–1491.
[15] Z.W. Zhang, G. Zhi, N. Qiao, Z.L. Kang, Z.L. Chen, L.M. Hu, Z.M. Yang, Y. Li, Copper-induced spermatozoa head malformation is related to oxidative damage to testes in CD-1 mice, Biol. Trace Elem. Res. 173 (2) (2016) 427–432.
[16] H. Guo, Y. Ouyang, J. Wang, H. Cui, H. Deng, X. Zhong, Z. Jian, H. Liu, J. Fang, Z. Zuo, X. Wang, L. Zhao, Y. Geng, P. Ouyang, H. Tang, Cu-induced spermatogenesis disease is related to oxidative stress-mediated germ cell apoptosis and DNA damage, J. Hazard Mater. (2021), 125903.
[17] J. Xue, F. Gruber, E. Tschachler, Y. Zhao, Crosstalk between Oxidative Stress, Autophagy and Apoptosis in Hemoporfin Photodynamic Therapy Treated Human Umbilical Vein Endothelial Cells, Photodiagnosis Photodyn Ther, 2020, 102137.
[18] N. Mizushima, M. Komatsu, Autophagy: renovation of cells and tissues, Cell 147 (4) (2011) 728–741.
[19] H. Liu, H. Deng, H. Cui, Z. Jian, H. Guo, J. Fang, Z. Zuo, J. Deng, Y. Li, X. Wang, L. Zhao, Copper induces hepatocyte autophagy via the mammalian targets of the rapamycin signaling pathway in mice, Ecotoxicol. Environ. Saf. 208 (2021), 111656.
[20] Q. Li, J. Liao, C. Lei, J. Shi, H. Zhang, Q. Han, J. Guo, L. Hu, Y. Li, J. Pan, Z. Tang, Metabolomics analysis reveals the effect of copper on autophagy in myocardia of pigs, Ecotoxicol. Environ. Saf. 213 (2021), 112040.
[21] F. Wan, G. Zhong, Z. Ning, J. Liao, W. Yu, C. Wang, Q. Han, Y. Li, J. Pan, Z. Tang, R. Huang, L. Hu, Long-term exposure to copper induces autophagy and apoptosis through oxidative stress in rat kidneys, Ecotoxicol. Environ. Saf. 190 (2020), 110158.
[22] X. Zhang, Y. Deng, J. Xiang, H. Liu, J. Zhang, J. Liao, K. Chen, B. Liu, J. Liu, Y. Pu, Galangin improved non-alcoholic fatty liver disease in mice by promoting autophagy, Drug Des. Dev. Ther. 14 (2020) 3393–3405.
[23] M.M. Ommati, R. Heidari, A. Jamshidzadeh, M.J. Zamiri, Z. Sun, S. Sabouri, J. Wang, F. Ahmadi, N. Javanmard, K. Seifi, S. Mousapour, B.S. Yeganeh, Dual effects of sulfasalazine on rat sperm characteristics, spermatogenesis, and steroidogenesis in two experimental models, Toxicol. Lett. 284 (2018) 46–55.
[24] T.D. Schmittgen, K.J. Livak, Analyzing real-time PCR data by the comparative C(T) method, Nat. Protoc. 3 (6) (2008) 1101–1108.
[25] J. Liu, F. Kuang, G. Kroemer, D.J. Klionsky, R. Kang, D. Tang, Autophagy-dependent ferroptosis: machinery and regulation, Cell. Chem. Biol. 27 (4) (2020) 420–435.
[26] I. Scheiber, R. Dringen, J.F. Mercer, Copper: effects of deficiency and overload, Met. Ions Life Sci. 13 (2013) 359–387.
[27] H. Guo, Y. Ouyang, J. Wang, H. Cui, H. Deng, X. Zhong, Z. Jian, H. Liu, J. Fang, Z. Zuo, X. Wang, L. Zhao, Y. Geng, P. Ouyang, H. Tang, Cu-induced spermatogenesis disease is related to oxidative stress-mediated germ cell apoptosis and DNA damage, J. Hazard Mater. 416 (2021), 125903.
[28] M. Martiniakova, R. Omelka, A. Jancova, G. Formicki, R. Stawarz, M. Bauerova, Accumulation of risk elements in kidney, liver, testis, uterus and bone of free-living wild rodents from a polluted area in Slovakia, J. Environ. Sci. Health A Tox Hazard. Subst. Environ. Eng. 47 (9) (2012) 1202–1206.
[29] M.T. Kuo, Y.F. Huang, C.Y. Chou, H.H.W. Chen, Targeting the copper transport system to improve treatment efficacies of platinum-containing drugs in cancer chemotherapy, Pharmaceuticals (Basel) 14 (6) (2021).
[30] Y. Nose, B.E. Kim, D.J. Thiele, Ctr1 drives intestinal copper absorption and is essential for growth, iron metabolism, and neonatal cardiac function, Cell Metabol. 4 (3) (2006) 235–244.
[31] H. Pierson, H. Yang, S. Lutsenko, Copper transport and disease: what can we learn from organoids? Annu. Rev. Nutr. 39 (2019) 75–94.
[32] M.H. Arafa, D.M. Amin, G.M. Samir, H.H. Atteia, Protective effects of tribulus terrestris extract and angiotensin blockers on testis steroidogenesis in copper overloaded rats, Ecotoxicol. Environ. Saf. 178 (2019) 113–122.
[33] M. Khushboo, M.K. Murthy, M.S. Devi, S. Sanjeev, K.S. Ibrahim, N.S. Kumar, V. K. Roy, G. Gurusubramanian, Testicular toxicity and sperm quality following copper exposure in Wistar albino rats: ameliorative potentials of L-carnitine, Environ. Sci. Pollut. Res. Int. 25 (2) (2018) 1837–1862.
[34] X. Tan, H. Guan, Y. Yang, S. Luo, L. Hou, H. Chen, J. Li, Cu(II) disrupts autophagy-mediated lysosomal degradation of oligomeric Aβ in microglia via mTOR-TFEB pathway, Toxicol. Appl. Pharmacol. 401 (2020), 115090.
[35] H. Zischka, G. Kroemer, Copper - a novel stimulator of autophagy, Cell Stress 4 (5) (2020) 92–94.
[36] Y. Shao, H. Zhao, Y. Wang, J. Liu, H. Zong, M. Xing, Copper-mediated mitochondrial fission/fusion is associated with intrinsic apoptosis and autophagy in the testis tissues of chicken, Biol. Trace Elem. Res. 188 (2) (2019) 468–477.
[37] Z. Kang, N. Qiao, G. Liu, H. Chen, Z. Tang, Y. Li, Copper-induced apoptosis and autophagy through oxidative stress-mediated mitochondrial dysfunction in male germ cells, Toxicol. Vitro 61 (2019), 104639.
[38] J. Liao, F. Yang, W. Yu, N. Qiao, H. Zhang, Q. Han, L. Hu, Y. Li, J. Guo, J. Pan, Z. Tang, Copper induces energy metabolic dysfunction and AMPK-mTOR pathway-mediated autophagy in kidney of broiler chickens, Ecotoxicol. Environ. Saf. 206 (2020), 111366.
[39] Y. Fang, C. Xing, X. Wang, H. Cao, C. Zhang, X. Guo, Y. Zhuang, R. Hu, G. Hu, F. Yang, Activation of the ROS/HO-1/NQO1 signaling pathway contributes to the copper-induced oxidative stress and autophagy in duck renal tubular epithelial cells, Sci. Total Environ. 757 (2020), 143753.
[40] J.Y. Liu, X. Yang, X.D. Sun, C.C. Zhuang, F.B. Xu, Y.F. Li, Suppressive effects of copper sulfate accumulation on the spermatogenesis of rats, Biol. Trace Elem. Res. 174 (2) (2016) 356–361.
[41] I. Seven, P. Tatli Seven, B. Gul Baykalir, T. Parlak Ak, S. Ozer Kaya, M. Yaman, Bee glue (propolis) improves reproductive organs, sperm quality and histological changes and antioxidant parameters of testis tissues in rats exposed to excess copper, Andrologia 52 (4) (2020), e13540.
[42] F. Yang, J. Liao, R. Pei, W. Yu, Q. Han, Y. Li, J. Guo, L. Hu, J. Pan, Z. Tang, Autophagy attenuates copper-induced mitochondrial dysfunction by regulating oxidative stress in chicken hepatocytes, Chemosphere 204 (2018) 36–43.
[43] X. Wu, X. Xue, L. Wang, W. Wang, J. Han, X. Sun, H. Zhang, Y. Liu, X. Che, J. Yang, C. Wu, Suppressing autophagy enhances disulfiram/copper-induced apoptosis in non-small cell lung cancer, Eur. J. Pharmacol. 827 (2018) 1–12.
[44] B. Zhou, J. Liu, R. Kang, D.J. Klionsky, G. Kroemer, D. Tang, Ferroptosis is a type of autophagy-dependent cell death, Semin. Cancer Biol. 66 (2020) 89–100.
[45] W. Hou, Y. Xie, X. Song, X. Sun, M.T. Lotze, H.J. Zeh 3rd, R. Kang, D. Tang, Autophagy promotes ferroptosis by degradation of ferritin, Autophagy 12 (8) (2016) 1425–1428.